LAWRENCE
LIVERMORE
NATIONAL
LABORATORY

LLNL-TR-678288

Generalized Rate Theory for Void and Bubble Swelling and its Application to Plutonium Metal Alloys

P. G. Allen, W. G. Wolfer

October 16, 2015

Disclaimer

This document was prepared as an account of work sponsored by an agency of the United States government. Neither the United States government nor Lawrence Livermore National Security, LLC, nor any of their employees makes any warranty, expressed or implied, or assumes any legal liability or responsibility for the accuracy, completeness, or usefulness of any information, apparatus, product, or process disclosed, or represents that its use would not infringe privately owned rights. Reference herein to any specific commercial product, process, or service by trade name, trademark, manufacturer, or otherwise does not necessarily constitute or imply its endorsement, recommendation, or favoring by the United States government or Lawrence Livermore National Security, LLC. The views and opinions of authors expressed herein do not necessarily state or reflect those of the United States government or Lawrence Livermore National Security, LLC, and shall not be used for advertising or product endorsement purposes.

This work performed under the auspices of the U.S. Department of Energy by Lawrence Livermore National Laboratory under Contract DE-AC52-07NA27344.

Disclaimer

This document was prepared as an account of work sponsored by an agency of the United States government. Neither the United States government nor Lawrence Livermore National Security, LLC, nor any of their employees makes any warranty, expressed or implied, or assumes any legal liability or responsibility for the accuracy, completeness, or usefulness of any information, apparatus, product, or process disclosed, or represents that its use would not infringe privately owned rights. Reference herein to any specific commercial product, process, or service by trade name, trademark, manufacturer, or otherwise does not necessarily constitute or imply its endorsement, recommendation, or favoring by the United States government or Lawrence Livermore National Security, LLC. The views and opinions of authors expressed herein do not necessarily state or reflect those of the United States government or Lawrence Livermore National Security, LLC, and shall not be used for advertising or product endorsement purposes.

This work performed under the auspices of the U.S. Department of Energy by Lawrence Livermore National Laboratory under Contract DE-AC52-07NA27344.

Generalized Rate Theory for Void and Bubble Swelling and its Application to Plutonium Metal Alloys

W.G. Wolfer and P.G. Allen, Lawrence Livermore National Laboratory, Livermore CA

Introduction

In the classical rate theory for void swelling, vacancies and self-interstitials are produced by radiation in equal numbers, and in addition, thermal vacancies are also generated at the sinks, primarily at edge dislocations, at voids, and at grain boundaries. In contrast, due to the high formation energy of self-interstitials for normal metals and alloys, their thermal generation is negligible, as pointed out by Bullough and Perrin [1]. However, recent DFT calculations of the formation energy of self-interstitial atoms in bcc metals [2,3] have revealed that the sum of formation and migration energies for self-interstitials atoms (SIA) is of the same order of magnitude as for vacancies. This is illustrated in Fig. 1 that shows the ratio of the activation energies for thermal generation of SIA and vacancies. For fcc metals, this ratio is around three, but for bcc metals it is around 1.5. Reviewing theoretical predictions of point defect properties in δ-Pu [4], this ratio could possibly be less than one. As a result, thermal generation of SIA in bcc metals and in plutonium must be taken into considerations when modeling the growth of voids and of helium bubbles, and the classical rate theory (CRT) for void and bubble swelling must be extended to a generalized rate theory (GRT).

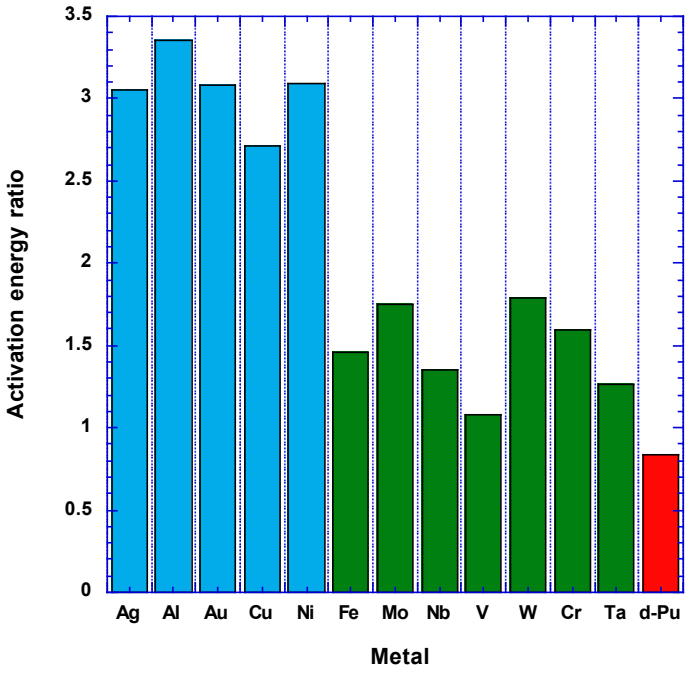

Fig.1. Ratio of SIA formation plus migration energy divided by self-diffusion energy

Structural materials contain elements that transmute to radioactive species when exposed to neutrons in nuclear reactors, and they may subsequently decay by emission of an α-particle. The helium atom produced by the radioactive decay also generates additional radiation-induced defects, and becomes then trapped in one vacancy, diffuses with it until captured by voids and bubbles, or until it recombines with a SIA. When the latter happens, the helium atom is promoted to an interstitial site, and it diffuses as an interstitial impurity at a much faster rate than the substitutional helium in a vacancy. It either becomes captured at voids or bubbles, or it finds another empty vacancy and converts back to a substitutional helium. The end result is that helium acquires an effective diffusion coefficient that determines the net capture at voids or bubbles, but it will be shown that it needs not be specified in the GRT.

In δ-Pu, the formation energy for SIA is so low that an interstitial helium is unstable and will create spontaneously a Frenkel pair, namely a SIA and a vacancy that it occupies.

As a result, a generalized rate theory (GRT) is needed for δ-Pu that includes three species produced by radiation and being captured at sinks, namely self-interstitials, mono-vacancies, and vacancies containing a helium atom, and two of these species, namely self-interstitials and vacancies, can also be re-emitted by the sinks via thermal activation.

Derivation of Generalized Rate Theory

Let G represent the total generation rate of vacancies and self-interstitials in collision cascades, and assign fG as the fraction of G that escapes cascades as migrating defects. Then the radiation-induced generation rates of self-interstitials, of vacancies, and of helium are fG, (f-1/n)G, and G/n, respectively. Here, n is the number of displacements of atoms generated by one a-decay. Appendix A provides details on how to compute both G and n. Kubota [5] has carried out molecular dynamics simulations of 20 keV collision cascades in Pu-Ga alloys at 600 K and found a small surviving fraction of only about 50 pairs of vacancies and self-interstitials that indicates that f = 0.1. At lower temperatures, however, f could be larger, and a value of f = 0.2 will be adopted for our calculations.

The rates of adsorption as well as of re-emission are proportional to the respective sink strength; the sink strength for edge dislocations is defined as

$$s_d = \frac{2\pi\rho_d}{\ell n[R_d / r_d]} \tag{1}$$

where ρ_d is the dislocation density, $r_d \approx 2b$ is the dislocation core radius, and

$$2R_d = 2/\sqrt{\pi\rho_d} \tag{2}$$

is the average separation distance between dislocations. The sink strength for bubbles with an average radius R_b is given by

$$s_b = 4\pi R_b n_b \tag{3}$$

where n_b is the number of bubbles per unit volume.

During the almost constant α-decay and perpetual defect generation, average concentrations of C_i, C_v, and C_{He} for self-interstitials, vacancies, and helium atoms, respectively, are established within the crystalline metal, and balanced by the losses to sinks. For this quasi-steady-state, the rate equations are

$$f\,G - \kappa\, D_i C_i D_v C_v - (Z_d^i s_d + Z_b^i s_b) D_i C_i + D_i (Z_d^i s_d C_i^d + Z_b^i s_b C_i^b) = 0 \qquad (4)$$

$$(f - 1/n) G - \kappa D_v C_v D_i C_i - (Z_d^v s_d + Z_b^v s_b) D_v C_v + D_v (Z_d^v s_d C_v^d + Z_b^v s_b C_v^b) = 0 \qquad (5)$$

$$G/n - Z_b^{He} s_b\, D_{He} C_{He} = 0 \qquad (6)$$

Eq. (6) reflect the fact that helium becomes absorbed by bubbles only, and once in bubbles, will not be re-emitted into the surrounding crystal, because the activation energy for such a process is too large. The rate of helium arrival at the bubbles, the second term, is simply equal to the rate of helium generation, and this is the reason why the effective helium diffusion coefficient, D_{He} , need not be specified.

The rate equations (4) and (5) are coupled by the recombination rate, the second term, with the recombination coefficient given by [6]

$$\kappa \approx \frac{32\pi}{a_0^2}\left(\frac{1}{D_v} + \frac{1}{D_i}\right) \qquad (7)$$

where a_0 is the lattice parameter. The second terms in eqs. (4) and (5) represent the loss of self-interstitials and vacancies to the sinks, while the third terms are the respective thermal production terms. These terms are determined by local thermodynamic conditions at the sinks and are given below. Hence, the two unknown quantities, henceforth abbreviated by

$$\phi_i = D_i C_i \quad and \quad \phi_v = D_v C_v\,, \qquad (8)$$

are the positive solutions of eqs. (4) and (5). In order to present these solutions in a compact form, we introduce several abbreviations.

The total sink strengths for interstitial and vacancy absorption are

$$\sigma_i = Z_d^i s_d + Z_b^i s_b \quad and \quad \sigma_v = Z_d^v s_d + Z_b^v s_b\,, \qquad (9)$$

while for thermal re-emission they are

$$\Psi_i = D_i (Z_d^i s_d C_i^d + Z_b^i s_b C_i^b)/\sigma_i \quad and \quad \Psi_v = D_v (Z_d^v s_d C_v^d + Z_b^v s_b C_v^b)/\sigma_v\,, \qquad (10)$$

respectively. With these abbreviations, the positive solutions can be expressed as

$$\sigma_i \phi_i = \frac{W_i - \sigma_i \sigma_v}{2\kappa} + \frac{1}{2}\left(\Psi_i - \Psi_v\right) + \frac{G}{2n} \tag{11}$$

$$\sigma_v \phi_v = \frac{W_v - \sigma_i \sigma_v}{2\kappa} + \frac{1}{2}\left(\Psi_v - \Psi_i\right) - \frac{G}{2n} \tag{12}$$

where

$$W_i = \sqrt{4\kappa\sigma_i\sigma_v(fG + \Psi_i) + (\kappa G/n - \sigma_i\sigma_v + \kappa\Psi_i - \kappa\Psi_v)^2} \tag{13}$$

$$W_v = \sqrt{4\kappa\sigma_i\sigma_v(fG - G/n + \Psi_v) + (\kappa G/n + \sigma_i\sigma_v + \kappa\Psi_i - \kappa\Psi_v)^2} \tag{14}$$

The bubble swelling rate can now be computed as the difference in arrival rates of vacancies and interstitials at bubbles, plus the re-emission rate of self-interstitials minus the re-emission rate of vacancies from bubbles, and finally plus the rate of helium atoms arriving at bubbles.

This swelling rate then is

$$\frac{dS}{dt} = s_b R \frac{dR}{dt} = s_b \left\{ Z_b^v(\phi_v - D_v C_v^b) - Z_b^i(\phi_i - D_i C_i^b) \right\} + G/n \tag{15}$$

Before it can be integrated to obtain the combined void and bubble swelling, sink bias factors and thermal re-emission rates must be defined.

Sink Bias Factors

The elastic interaction of the migrating defects with the internal stress fields of dislocations and bubbles influences their diffusion. This elastic interaction is dependent on the relaxation volume of the defect. For vacancies, its relaxation volume is the reduction of the vacant lattice site due to the inward relaxation of the surrounding atoms, and for normal fcc metals it is typically about -0.2 Ω, where Ω is the volume per atom. For SIA, its relaxation volume is determined by the outward displacement of surrounding atoms, and in the case of Ni and stainless steels, it produces a relaxation volume of 1.8 Ω. As a result, SIA are preferentially migrating to dislocations. This preference is quantified by an interstitial bias factor for dislocation Z_i^d >1.

The theory for evaluating bias factors for dislocations has been reviewed by Wolfer [7]. For edge dislocations, the bias factor is given in terms of the modified Bessel functions K_0 and I_0 as:

$$Z_d(T, V^{rel}) = \ell n(R_d / r_d)\left[\frac{K_0(r_d^{cap}/R_d)}{I_0(r_d^{cap}/R_d)} - \frac{K_0(r_d^{cap}/r_d)}{I_0(r_d^{cap}/r_d)}\right]^{-1} \tag{16}$$

where the capture radius of the dislocation is defined as

$$r_d^{cap} = \frac{(1+\nu)b}{6\pi(1-\nu)} \frac{\mu \left| V^{rel} \right|}{kT} \tag{17}$$

and μ and ν are the shear modulus and Poisson's ratio, respectively, and *b* is the Burgers vector. A bias factor for a void or a bubble with radius R_b is due to the image interaction between the migrating defect and the cavity surface, given by:

$$U^{im}(r, R_b) = -\frac{(1+\nu)^2 \mu (V^{rel})^2}{36\pi(1-\nu) R_b^3} \sum_{n=2}^{\infty} \frac{n(n-1)(2n-1)(2n+1)}{n^2 + (1-2\nu)n + 1 - \nu} \left(\frac{R_b}{r} \right)^{2n+2} \tag{18}$$

where r is the distance between the cavity center and the defect. To obtain the bias factor

$$Z_b(T, V^{rel}, R_b) = \left[\int_0^1 \exp[U^{im}(r, R_b)/kT] \, d(R_b/r) \right]^{-1} \tag{19}$$

requires a numerical integration. Suhr and Wolfer [8] have developed an approximation for the infinite sum in eq.(18) that greatly facilitates this numerical integration. The numerical results can be represented using a capture coefficient of

$$\theta(T, V^{rel}) = \frac{(1+\nu)^2}{36\pi(1-\nu)} \frac{\mu (V^{rel})^2}{\Omega kT} \tag{20}$$

as $$Z_b(T, V^{rel}, R_b) \approx 1 + 1.0921 \theta^{0.54314} \, R_b^{-0.88727 \, \theta^{-0.021069}} \tag{21}$$

We evaluate the bias factors for nickel as it exhibits void swelling behavior similar to austenitic stainless steels for which extensive neutron radiation damage results exist. In addition, experimental values are available for the relaxation volume of self-interstitials, namely V_i^{rel} =1.8 Ω, and the one for vacancies, V_v^{rel} = 0.2 Ω.

Shear modulus and Poisson's ratio for Ni are μ = 94.6 GPa and ν = 0.287, respectively, and the Burgers vector is *b* = 0.249 nm. For a temperature of T = 723 K, bias factors are obtained as shown in Fig. 2.

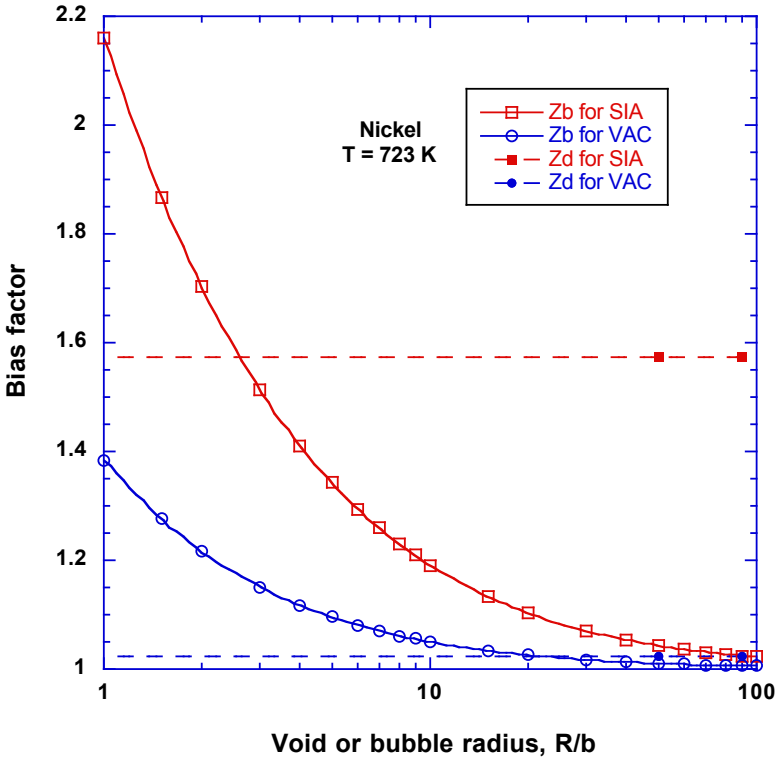

Figure 2. Bias factors of Ni for edge dislocations, Z_d, and for voids or bubbles, Z_b, as a function of their radii.

As shown in Fig. 2, the interstitial bias factor for voids or bubbles with diameters less than 2.5 nm is larger than the interstitial bias factor for edge dislocations. Bias-driven void growth in nickel is possible only for voids or bubbles with diameters larger than 2.5 nm.

To provide an example of the bias factors for δ-Pu (b = 0.33 nm), we select two possible values for the relaxation volumes, namely V_i^{rel} = 0.6 Ω and V_v^{rel} = -0.73 Ω, and a temperature of T = 350 K. As seen in Fig. 3 , the bias factors for self-interstitials and for vacancies are nearly the same, but vacancies are now attracted more to dislocations. This reversal implies that void swelling would not occur in d-Pu. But even if other possible values are selected more favorable to void swelling, i.e. $V_i^{rel} > |V_v^{rel}|$, it must be mentioned that void swelling depends on the net bias and on the ratio of sink strengths for voids and dislocations.

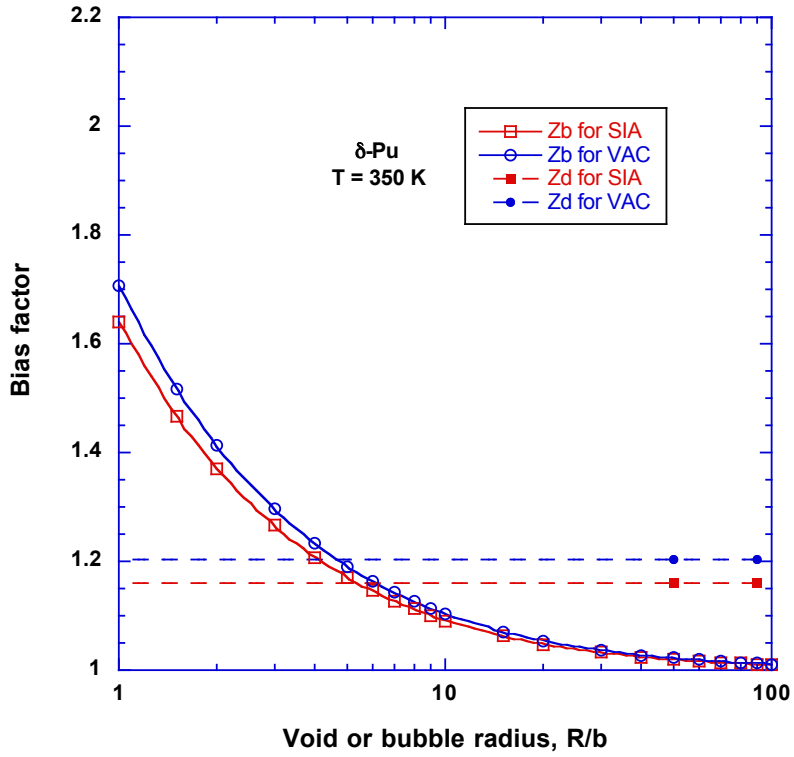

Figure 3. Bias factors of d-Pu for edge dislocations, Z_d , and for voids or bubbles, Z_b .

Thermodynamic Equilibrium Concentrations at Voids and Bubbles

The thermal re-emission rates of vacancies and of SIA from sinks are defined in eqs. (10), and they in turn depend on local thermodynamic equilibrium concentrations. Let us first consider the case of vacancies in local thermodynamic equilibrium with bubbles having a radius of R_b and filled with helium to a pressure of p. One then evaluates the change in Gibbs free energy when one vacancy is emitted from the bubble to the surrounding crystal lattice. This change is

$$\Delta G = -E_v^f + TS_v^f + \Delta F_S - p\Omega w - kT\ \ell n C_V^b \qquad (22)$$

Here, E_v^f and S_v^f are the vacancy formation energy and entropy, respectively, ΔF_S is the change in surface free energy, -$p\Omega w$ is the work performed by the gas, and the last term is the change in configurational entropy. The number n_b of host metal atoms missing in the bubble is given by

$$\tfrac{4\pi}{3} R_b^3 = n_b \Omega\,, \qquad (23)$$

so the change in the surface free energy can be written as

$$\Delta F_S(n_b) = F_S(n_b+1) - F_S(n_b) = (4\pi)^{1/3}(3\Omega)^{2/3}\left[(n_b+1)^{2/3} - n_b^{2/3}\right]\gamma_0 \cong \frac{2\gamma_0}{R_b}\Omega \qquad (24)$$

where γ_0 is the specific surface energy. The final result is the well-known capillary approximation for $n_b >> 1$ leading to the surface tension $2\gamma_0/R_b$. But as the derivation shows, the surface tension is not a mechanical force, but a thermodynamic or configurational force. For small bubbles, the capillary approximation will be avoided and the correct free energy change will be used instead. The correction factor w for the work performed by the gas is also required for small bubbles only as shown in Appendix B.

The local vacancy concentration in thermodynamic equilibrium with the bubble is now obtained when $\Delta G = 0$ as

$$C_V^b = C_V^{eq} \exp\left[\frac{\Delta F_S - p\Omega w}{kT}\right] \qquad (25)$$

The thermal vacancy concentration in the solid without bubbles or voids is

$$C_v^{eq} = C_v^d = \exp\left(-\frac{E_v^f}{kT} + \frac{S_v^f}{k}\right) \qquad (26)$$

In analogous fashion one can derive the concentration of SIA in thermal equilibrium with a bubble. However, since $\Delta F_S(n_b) = F_S(n_b\text{-}1) - F_S(n_b)$ and the gas is now further compressed when a surface atom is removed to create one SIA, there is a change in sign, and

$$C_i^b = C_i^{eq} \exp\left[\frac{p\Omega w - \Delta F_S}{kT}\right] \qquad (27)$$

with

$$C_i^{eq} = C_i^d = \exp\left(-\frac{E_i^f}{kT} + \frac{S_i^f}{k}\right) \qquad (28)$$

being the equilibrium concentration of SIA in the solid without voids or bubbles.

The helium pressure within small bubbles can reach high values that approach the phase transition to solid helium. Accurate equations of state for both gas and solid helium are presented in Appendix B and have been used in the prediction for bubble swelling in aged plutonium to be described in the next section.

Bubble and Void Swelling in Neutron Irradiated Steel

The numerical solution of the rate equations 4, 5 and 6, and the subsequent integration of the swelling rate equation 15 is accomplished with a GRT code using Mathematica. As a validation, the GRT code has been applied first to predict void swelling in a pure ternary alloy of Fe, Ni, and Cr (same composition as in austenitic steels but without carbon and minor constituents) under fast neutron irradiation of 21 dpa/year. Samples of these pure ternary alloys were irradiated in the FFTF and subsequently examined by TEM to determine void swelling [105].

Irradiation conditions and physical parameters are listed in Table 1.

Table 1. Properties for Ni and pure stainless steels irradiated in FFTF

Lattice parameter	0.352 nm
Shear modulus	91.3 GPa
Poison's ratio	0.276
Displacement rate	21 dpa/year
Fraction released from cascades	f = 0.7
Irradiation temperature	773 K
Dislocation density	10^{15} m^{-2}
Void density	10^{21} m^{-3}
Vacancy formation energy	1.79 eV
Vacancy migration energy	1.07 eV
Vacancy diffusion pre-factor	$9.2 \cdot 10^{-5}$ m^2 s^{-1}
Vacancy relaxation volume	-0.2 Ω
SIA formation energy	3.72 eV
SIA migration energy	0.15 eV
SIA diffusion pre-factor	10^{-7} m^2 s^{-1}
SIA relaxation volume	1.8 Ω

The void nucleation period in these pure ternary alloys is about 6 dpa, and the predicted void growth gives then rise to void swelling as shown by the dashed curve in Fig. 4. Measured void swelling determined by TEM observations [9] are also shown for two samples that were irradiated at displacement rates of 16.4 and 30.3 dpa/year. The agreement with the theoretical prediction carried out at the intermediate dose rate of 21 dpa/year is satisfactory.

Bubble Swelling in Delta Phase Plutonium

For the prediction of combined void and bubble swelling in gallium-stabilized plutonium we select as the starting point the TEM results of Schwartz et al. for a 42 year-old plutonium sample. Correcting the measured TEM image diameters upwards by 20% and assuming an actual bubble density somewhat higher than what is visible, all the helium produced can be accommodated in a bubble volume fraction of 0.05% and at a helium density of 2.5 He/Vac. To reach this state requires that the bubbles had to grow by thermal emission of SIA with a SIA formation energy of 1.25 eV and a SIA migration energy of 0.15 eV. Other materials parameters used to predict swelling beyond 42 years are listed in Table 2.

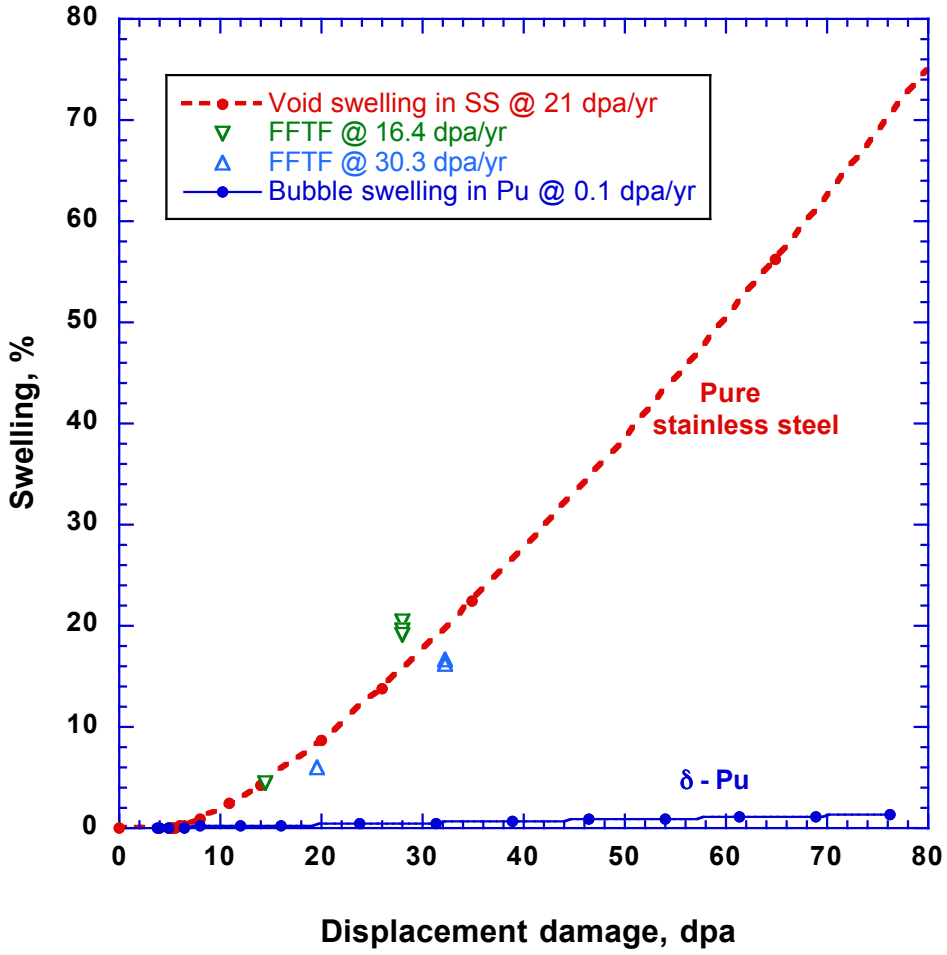

Figure 4. Void swelling observed and predicted (dashed line) in pure ternary stainless steel samples irradiated in FFTF compared to predicted swelling for 42 year-old Ga-stabilized δ-Pu.

Table 2. Parameters for aged delta plutonium

Lattice parameter	0.4637 nm
Shear modulus	17.3 GPa
Poisson's ratio	0.2605
Displacement rate	0.081 dpa/year
Fractional release from cascades	f = 0.2
Irradiation temperature	308 K
Dislocation density	10^{13} m^{-2}
Bubble density	$2 \cdot 10^{23}$ m^{-3}
Vacancy formation energy	0.75 eV
Vacancy migration energy	0.70 eV
Vacancy diffusion pre-factor	$4.5 \cdot 10^{-4}$ m^2 s^{-1}
Vacancy relaxation volume	-0.7 Ω
SIA formation energy	1.25 eV
SIA migration energy	0.15 eV
SIA diffusion pre-factor	10^{-7} m^2 s^{-1}
SIA relaxation volume	1.4 Ω

For the following GRT predictions, relaxation volumes of V_{SIA} = 1.4 Ω and V_{VAC} = -0.7 Ω are selected; in principle this should provide a sufficiently strong bias for preferential capture of SIA at dislocations and preferential capture of vacancies at bubbles. However, the GRT prediction displayed in Fig. 5 reveal that bias-driven swelling makes only a small contribution, namely the dotted curve, to the combined swelling shown as the solid curve. The dashed curve gives bubble swelling if the helium density had stayed at 2.5 He/Vac. Because of the bias-driven contribution, the helium density in the bubbles declines to a value of 2.415 He/Vac at an age of 1000 years or at 76 dpa.

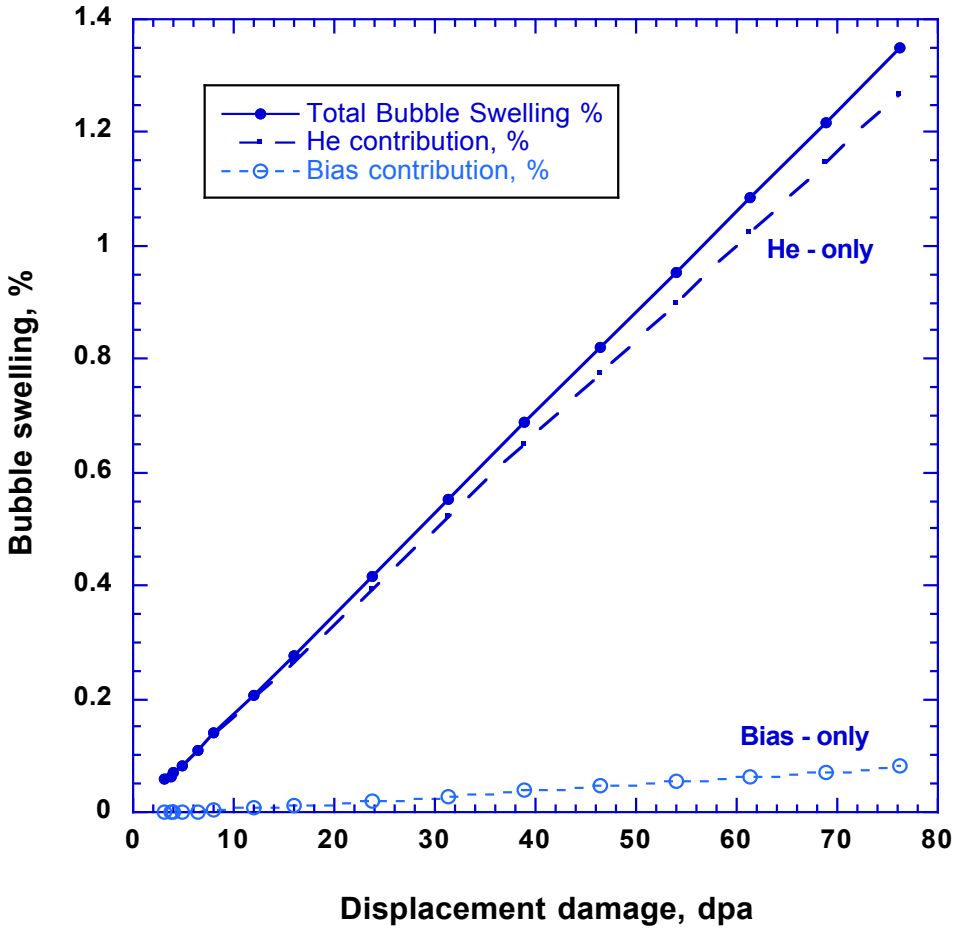

Figure 5. Predicted continuation of bubble swelling for a 42 year-old Ga-stabilized δ-Pu, and the contributions from helium-driven and bias-driven processes.

The dramatic difference between bubble swelling in δ-Pu and void swelling in regular fcc metals is mainly due to the overwhelmingly high bubble density in δ-Pu , $2 \cdot 10^{23}$ m^{-3}, compared to the void density of 10^{21} m^{-3} in irradiated stainless steels. The abundance of helium bubbles in δ-Pu as sinks for radiation-produced defects, in comparison to dislocation sinks, prevents any significant net bias to ever develop, regardless of the magnitude of the relaxation volumes for SIA and vacancies. As a result, the only available process for bubble growth under continuing helium production is the thermally activated emission of SIA from bubbles. The low formation energy of SIA in δ-Pu makes this a viable process, otherwise the helium pressure within bubbles would have to rise to about 3 He/Vac to induce emission of prismatic dislocation loops. However, no prismatic loops near bubbles have been found in TEM observations of aged δ-Pu.

References

1. R. Bullough, R.C. Perrin, "Theory of void formation and growth in irradiated materials", Proc. Of the 1971 Internat. Conf. on Radiation-Induced Voids in metals, eds. J.W. Corbett, L.C. Ianniello, CONF-71061, pp. 769-797

2. P.M. Derlet, D. Nguyen-Manh, S.L. Dudarev, Phys. Rev. **B76** (2007) 054107

3. S.L. Dudarev, Density Functional Theory Models for Radiation Damage, Annu. Rev. Mater. Res. **43** (2013) 35-61

4. W.G. Wolfer, P.G. Allen, "Review of Calculations on Point Defect Properties in Delta-Pu", LLNL-TR-676992, Sept. 8, 2015

5. A. Kubota, "Understanding the Atomic-Scale Aspects of Radiation Damage and Aging in Pu and Pu/Ga Alloys through Computer Simulations", LBNL seminar, Dec. 13, 2006

6. W.G. Wolfer, A. Si-Ahmed, J. Nucl. Mater. **99** (1981) 117

7. W.G. Wolfer, J. Computer-Aided Mater. Des. **14** (2007) 403

8. M.P. Surh, W.G. Wolfer, J. Computer-Aided Mater. Des. **14** (2007) 419

9. T. Okita, W. G. Wolfer, J. Nucl. Mater. **327**, 130-139 (2004)

Appendix A: Rates of Displacements and Helium Production

Weapons-grade plutonium contains several isotopes, and each isotope produces slightly different a-decay energies and partitions it to kinetic energies of helium and actinide daughter products. In turn, the kinetic energies are dissipated into an electronic and a nuclear stopping power, and the latter produces the collision cascades containing the Frenkel pairs. The combined numbers of Frenkel pairs from the collision cascades of the helium and the actinide daughter products is referred to as the number of displacements per atom (dpa) per a-decay. Table A1 contains the list of the main Pu isotopes, their initial atomic fractions N_X in weapons-grade plutonium, their half-lives t_X , the a-decay energies, and the dpa/decay, n_X .

Table A1.

Isotope	Fraction	Half-live (years)	Decay energy (MeV)	dpa/decay
Pu 238	0.0002	87.7	5.580	2726
Pu 239	0.936	24110	5.236	2572
Pu 240	0.059	6563	5.243	2569
Am 241	0.00044	432.7	5.571	2700

The rate of helium generation, expressed in atomic fractions per year, is given by

$$G_{He}(t) = \ell n(2) \sum_{X=238}^{241} \frac{N_X}{t_X} \exp\left(-\frac{t}{t_X}\right) \qquad \text{(A1)}$$

Multiplying each term with the corresponding N_X produces the formula for the generation rate of Frenkel pairs, again in atomic fractions per year:

$$G(t) = \ell n(2) \sum_{X=238}^{241} \frac{N_X n_X}{t_X} \exp\left(-\frac{t}{t_X}\right) \qquad \text{(A2)}$$

The number of Frenkel pairs produced per a-decay is then

$$n(t) = G(t) / G_{He}(t) \qquad \text{(A3)}$$

and it is shown in Fig. A1. As can be seen, it is not quite a constant, but it decreases only by about 0.35 % over 500 years.

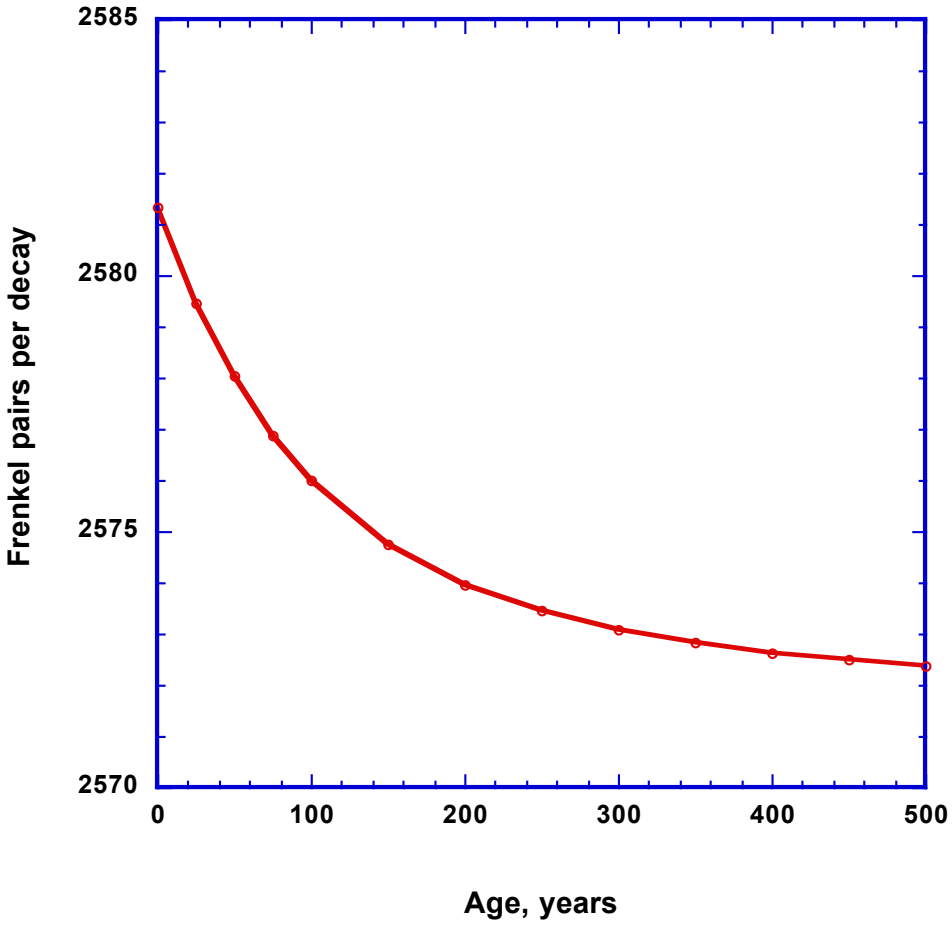

Fig. A1. The change of the Frenkel pair production per decay with time.

Appendix B:

The Equations of State for Helium in the Solid and Fluid Phases

The density of helium in bubbles found in aged metal tritides ranges from about 0.07 to 0.25 mol/cm^3. At ambient temperatures, the helium pressure in the very small bubbles (diameter of 1nm or less) reaches about 10 GPa, which is close to the phase transition between fluid and solid helium. It is therefore necessary to utilize equations of state for both the fluid and the solid states.

A matching set of equations of state (EOS) had been developed earlier by Wolfer et al. (1984, 1988) based on the available experimental data tabulated by McCarty (1973). At the time, however, no data were available close to the region of phase transition from fluid to solid. In the meantime, such data have been obtained and published (Polian et al., 1983; Mao et al., 1988; Loubeyre et al., 1993).

Examination of these data at T=300 K has shown that the solid EOS agrees well with the newer data, and a minor adjustment of some parameters in the fluid EOS leads to a new, excellent fit. This is shown in Figure B1.

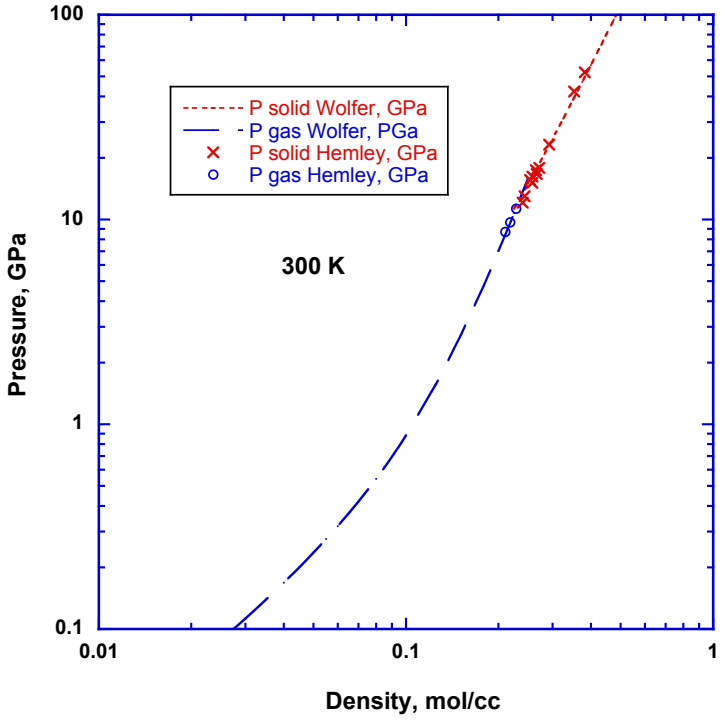

Fig. B1. Helium pressure at 300 K versus density for fluid and solid phases

The new EOS for helium is given in terms of the compressibility factor

$$z(\mu,T) = 10^3 \frac{p}{\mu RT} \tag{B1}$$

where m is the helium density in mol/cm^3, p is the pressure in units of GPa, and R = 8.314 J/mol/K is the gas constant. The compressibility factors for both the fluid and the solid phases, z_g and z_S, are expressed as power series in the density as

$$z(\mu,T) = C_0(T) + C_1(T)\,(100\,\mu) + C_2(T)\,(100\,\mu)^2 + C_3(T)\,(100\,\mu)^3 \tag{B2}$$

with the following temperature dependent coefficients. For the fluid phase,

$$\begin{aligned} C_0^g(T) &= \left(T/1300\right)^{0.04} \\ C_1^g(T) &= 5.83/(T+14)^{0.58} \\ C_2^g(T) &= \frac{\log_{10}[(T+42)/800]}{0.69(T+42)^{0.65}} \\ C_3^g(T) &= 0.86/(T+70)^{1.44} \end{aligned} \tag{B3}$$

and for the solid phase,

$$\begin{aligned} C_0^s(T) &= -3.89 + 6.59\,(T/100) - 1.15\,(T/100)^2 + 0.0546\,(T/100)^3 \\ C_1^s(T) &= -0.523 - 0.439\,(T/1000) + 1.77\,(T/1000)^2 - 1.39\,(T/1000)^3 \\ C_2^s(T) &= 0.101 - 0.291\,(T/1000) + 0.301\,(T/1000)^2 - 0.1045\,(T/1000)^3 \\ C_3^s(T) &\approx 0 \end{aligned} \tag{B4}$$

The intersection of the two compressibility factors, i.e. when $z_g(\mu_m,T_m) = z_S(\mu_m,T_m)$, defines approximately melt densities and melt temperatures. However, it neglects a small density difference between the fluid and solid phase, or a small density range over which mixtures of the two phases coexists. Accepting this minor inaccuracy, the following correlation is obtained:

$$\mu_m \approx 0.0269\,T_m^{0.359} + 1.953\cdot 10^{-7}\,T_m^{1.903} \quad mol/cm^3 \tag{B5}$$

For many uses, including ours here, it is of advantage to express the compressibility factor as a function of pressure and temperature. The following empirical correlation has been

developed for the compressibility factor of fluid helium in the temperature range of 200 K $\leq$ T$\leq$ 700 K:

$$z_g(p,T) \approx 1 + Z(T)\, p^{\xi(T)} \qquad \text{(B6)}$$

with

$$Z(T) = -0.12713 + 874.84 / T \qquad \text{(B7)}$$

and

$$\xi(T) = 0.82818 - 12.375 / T + 715.17 / T^2 \qquad \text{(B8)}$$

In the relationship (B6), the fluid pressure is given in units of GPa. Within the pressure range of 0.5 GPa to 10 GPa, the compressibility factor obtained from (B6) deviates from the more exact result (B2) by no more than 4 %.

Using the expression (B2) for z_g and z_s , one can obtain the compressibilities and their inverse, namely the bulk moduli. They are shown for T = 300 K in Fig. B2.

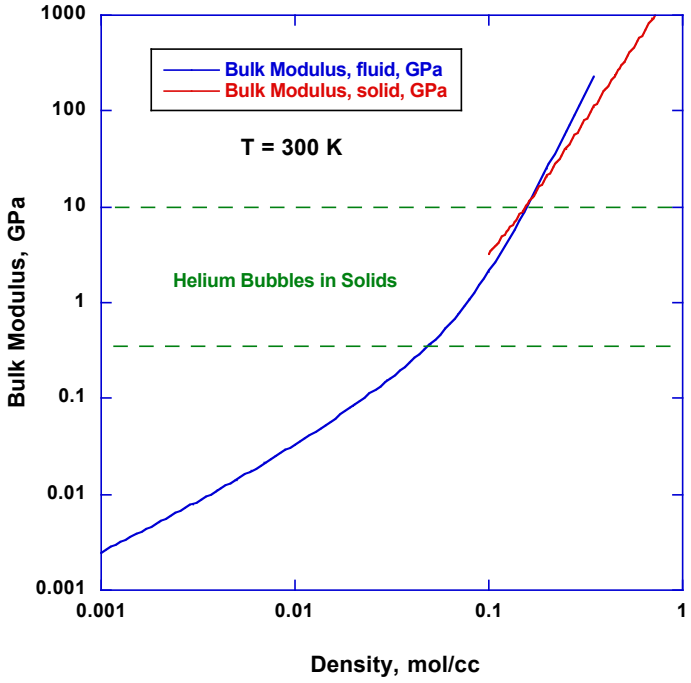

Fig. B2. Bulk modulus for liquid and solid helium at T = 300 K.

Appendix B References

1. Loubeyre, P., LeToullec, R., Pinceaux, J.P., Mao, H.K., Hu, J., Hemley, R.J., 1993. Phys. Rev. Letters 71, 2272.

2. Mao, H.K., Hemley, R.J., Jephcoat, A.P., Finger, L.W., Zha, C.S., Bassett, A., 1988. Phys. Rev. Letters 60, 2649.

3. McCarty, R.D., 1973. *Thermodynamic Properties of Helium 4 from 2 to 1500 K at Pressures to 10^8 Pa.* J. Phys. Chem. Ref. Data **3**, 923-958.

4. Polian, A., Grimsditch, M., 1983, Europhys. Letters 2, 849.

5. Wolfer, W.G., Glasgow, B.B., Wehner, M.F., Trinkaus, H., 1984. *Helium equation of state for small cavities: Recent developments.* J. Nucl. Mater. **123&124**, 565-570.

6. Wolfer, W.G., 1988. *The pressure for dislocation loop punching by a single bubble. Phil. Mag.* **58**, 285-297

7. Wolfer, W.G., 1989. *Dislocation loop punching in bubble arrays. Phil. Mag.* **59**, 87-103